

# CDC42-related genes are upregulated in helper T cells from obese asthmatic children



Deepa Rastogi, MBBS, MS,<sup>a</sup> John Nico, BS,<sup>a</sup> Andrew D. Johnston, MS,<sup>b</sup> Toni Adrienne M. Tobias, BA,<sup>a</sup> Yurydia Jorge, MD,<sup>a</sup> Fernando Macian, MD, PhD,<sup>c</sup> and John M. Greally, DMed, PhD<sup>b</sup> *Bronx, NY*

**Background:** Pediatric obesity-related asthma is more severe and less responsive to medications than asthma in normal-weight children. Obese asthmatic children have nonatopic T<sub>H</sub>1-polarized systemic inflammation that correlates with pulmonary function deficits, but the pathways underlying T<sub>H</sub>1-polarized inflammation are not well understood.

**Objective:** We compared the CD4<sup>+</sup> T-cell transcriptome in obese children with asthma with that in normal-weight children with asthma to identify key differentially expressed genes associated with T<sub>H</sub>1-polarized inflammation.

**Methods:** CD4<sup>+</sup> T-cell transcriptome-wide differential gene expression was compared between 21 obese and 21 normal-weight children by using directional RNA sequencing. High-confidence differentially expressed genes were verified in the first cohort and validated in a second cohort of 20 children (10 obese and 10 normal-weight children) by using quantitative RT-PCR.

**Results:** Transcriptome-wide differential gene expression among obese asthmatic children was enriched for genes, including *VAV2*, *DOCK5*, *PAK3*, *PLD1*, *CDC42EP4*, and *CDC42PBB*, which are associated with CDC42, a small guanosine triphosphate protein linked to T-cell activation. Upregulation of *MLK3* and *PLD1*, genes downstream of CDC42 in the mitogen-activated protein kinase and mammalian target of rapamycin pathways and the inverse correlation of *CDC42EP4* and *DOCK5* transcript counts with FEV<sub>1</sub>/FVC ratio together support a role of CDC42 in the T<sub>H</sub>1 polarization and pulmonary function deficits found in patients with obesity-related asthma.

**Conclusions:** Our study identifies the CDC42 pathway as a novel target that is upregulated in T<sub>H</sub> cells of obese asthmatic children, suggesting its role in nonatopic T<sub>H</sub>1-polarized systemic

inflammation and pulmonary function deficits found in patients with pediatric obesity-related asthma. (*J Allergy Clin Immunol* 2018;141:539-48.)

**Key words:** Asthma, obesity, helper T cell transcriptome, children

Obesity and asthma are 2 of the most common pediatric diseases, particularly among African American and Hispanic subjects.<sup>1,2</sup> Obesity is a known predictor of childhood asthma,<sup>3</sup> and obesity-related asthma is distinct from asthma in normal-weight patients.<sup>4</sup> Obese children with asthma have higher disease morbidity,<sup>5</sup> lower pulmonary function,<sup>6</sup> and lower responsiveness to bronchodilators compared with normal-weight children with asthma.<sup>7</sup> Although truncal adiposity<sup>8</sup>; metabolic abnormalities, including insulin resistance and dyslipidemia<sup>9,10</sup>; and systemic inflammation<sup>6</sup> have been postulated, the precise mechanisms underlying pediatric obesity-related asthma are not well elucidated.

Obese asthmatic children have evidence of nonatopic T<sub>H</sub>1-polarized systemic inflammation,<sup>6,11</sup> which is associated with pulmonary function deficits<sup>6,11</sup> and differs from atopic inflammation associated with classic childhood asthma.<sup>12</sup> Moreover, insulin resistance mediates the association of T<sub>H</sub>1 polarization with pulmonary function deficits.<sup>11</sup> Although extensive investigation of immune pathways in the context of atopic asthma<sup>13</sup> has led to the development of targeted therapy, including omalizumab,<sup>14</sup> the lack of a similar understanding of mechanisms underlying nonatopic immune responses, as observed in the context of obesity-related asthma,<sup>6,11</sup> is associated with limited therapeutic options for obese children with asthma.

To address these gaps in knowledge, we compared the CD4<sup>+</sup> (T<sub>H</sub>) cell transcriptome of obese asthmatic children with that of normal-weight asthmatic children of African American and Hispanic ethnicity to elucidate the mechanistic immune pathways underlying T<sub>H</sub>1 polarization. We hypothesized that gene expression in CD4<sup>+</sup> T cells from obese asthmatic patients differs from that in normal-weight asthmatic patients, and its investigation will allow for identification of key molecules underlying the nonatopic T<sub>H</sub>1-polarized inflammation associated with the obese asthma phenotype.

## METHODS

### Study population

Two study cohorts comprised of obese and normal-weight African American and Hispanic children aged 7 to 11 years with asthma were recruited from clinics at Children's Hospital at Montefiore between July 2013 to June 2016. The first discovery cohort comprised 42 children, including 21 obese and 21 normal-weight children with asthma. The second validation cohort comprised 20 children, including 10 obese and 10 normal-weight children with asthma. Obesity was defined as a body mass index of greater than the 95th percentile for age and sex. Asthma was classified based on the clinical diagnosis made by a health care provider that was confirmed on

From the Departments of <sup>a</sup>Pediatrics, <sup>b</sup>Genetics, and <sup>c</sup>Pathology, Albert Einstein College of Medicine.

Supported in part by K23 HL118733 (to D.R.), the Feldstein Medical Foundation, National Institutes of Health/National Center for Research Resources CTSA grant 1 UL1 TR001073-01, 1 TL1 TR001072-01, and 1 KL2 TR001071-01 (Albert Einstein Institute of Clinical and Translational Research) from the National Center for Advancing Translational Sciences (NCATS), a component of the NIH. The views expressed in this article do not communicate an official position of the NIH/NCRR.

Disclosure of potential conflict of interest: D. Rastogi receives grant support from the National Heart, Lung, and Blood Institute. F. Macian receives grant funding from Medivation. J. M. Greally receives grant funding from the National Institutes of Health and is an employee of Albert Einstein College of Medicine. The rest of the authors declare that they have no relevant conflicts of interest.

Received for publication September 28, 2016; revised April 4, 2017; accepted for publication April 18, 2017.

Available online May 4, 2017.

Corresponding author: Deepa Rastogi, MBBS, MS, Children's Hospital at Montefiore, Albert Einstein College of Medicine, 3415 Bainbridge Ave, Bronx, NY 10467. E-mail: drastogi@montefiore.org.

© The CrossMark symbol notifies online readers when updates have been made to the article such as errata or minor corrections

0091-6749/\$36.00

© 2017 American Academy of Allergy, Asthma & Immunology

<http://dx.doi.org/10.1016/j.jaci.2017.04.016>

**Abbreviations used**

FRC:	Functional residual capacity
FVC:	Forced vital capacity
GTP:	Guanosine triphosphate
MAPK:	Mitogen-activated protein kinase
mTOR:	Mammalian target of rapamycin
qRT-PCR:	Quantitative RT-PCR
RNA-seq:	RNA sequencing
RV:	Residual volume
TLC:	Total lung capacity

electronic medical records. All participants completed a research study visit at the Clinical Research Center at the Montefiore Medical Center where they underwent anthropometric measurements, allergy skin prick testing to 8 allergens (tree mix, grass mix, ragweed, dust mite [*Dermatophagoides pteronyssinus*], cockroach, mouse, cat, and mold), and fasting phlebotomy, as previously described.<sup>6</sup> Pulmonary function testing was abstracted from the medical charts. It was performed per American Thoracic Society guidelines and included spirometry and lung volume quantification by nitrogen washout, as previously described.<sup>6</sup> Percent predicted values were calculated for spirometric indices by using the National Health and Nutrition Examination Survey prediction equations and for lung volume indices by using equations developed by the American Thoracic Society workshop, as previously described.<sup>6</sup> The institutional review board at Albert Einstein College of Medicine approved the study.

**Study measures**

**Separation of CD4<sup>+</sup> T cells.** Given the association of insulin resistance with T<sub>H</sub>1 polarization,<sup>11</sup> we processed fasting blood for cell and serum separation. PBMCs were separated by using the Ficoll Hypaque method. CD4<sup>+</sup> T cells were isolated from PBMCs by means of negative selection with magnetic beads (EasySep; Stem Cell Technologies, Tukwila, Wash) to avoid any *ex vivo* CD4<sup>+</sup> T-cell stimulation. The CD4<sup>+</sup> T-cell purity was 95% to 98%, as confirmed by means of flow cytometry (see Fig E1 in this article's Online Repository at [www.jacionline.org](http://www.jacionline.org)). T-cell proportions did not differ between the obese (26.6% ± 5%) and normal-weight (27.1% ± 7.4%) samples. Unstimulated T cells were used for transcriptome quantification to elucidate differential gene expression more reflective of *in vivo* conditions. Serum separated from fasting blood was used for insulin quantification by using a radioimmunoassay (Millipore, Temecula, Calif) on a Wizard2 gamma counter (PerkinElmer, Waltham, Mass). Lipids were quantified by using an enzymatic immunoassay and measured on an AU400 Chemistry Autoanalyzer (Beckman Coulter, Fullerton, Calif).

**CD4<sup>+</sup> T-cell transcriptome quantification by means of directional RNA sequencing.** Expression levels of genes in the CD4<sup>+</sup> T-cell transcriptome were quantified in the discovery cohort of 42 participants. CD4<sup>+</sup> T-cell RNA from the validation cohort of 20 participants was used to validate the transcriptome findings from the discovery cohort. RNA extracted from 2 × 10<sup>6</sup> CD4<sup>+</sup> T cells with QIAzol (Qiagen, Valencia, Calif) underwent quality control testing (2100 Bioanalyzer; Agilent Technologies, Santa Clara, Calif), and samples with RNA integrity number of 8 or greater underwent processing for directional RNA sequencing (RNA-seq) library preparation. After removal of ribosomal RNA with the Ribo Zero-rRNA removal kit (Illumina, San Diego, Calif), reverse transcription was performed with the SuperScript III First-Strand Synthesis System (Thermo Fisher Scientific, Waltham, Mass), followed by second-strand cDNA synthesis with dUTP (Thermo Fisher Scientific). Double-stranded cDNA was fragmented with Covaris-Focused ultrasonicator (Covaris Inc, Woburn, Mass; 200- to 300-bp target length), end-repaired, and dA tailed, and adaptors were added for the Illumina sequencer to allow multiplexing of 8 samples per lane. A combination of dUTP incorporation and uracil-DNA glycosylase was used to maintain directional information (ie, transcribing strand-specific information).<sup>15</sup> All libraries underwent

Bioanalyzer testing for quality control and were sequenced on the Illumina HiSeq 2500 as 100-bp single-end reads.

**Alignment and analysis of directional RNA-seq libraries.** All bioinformatics analyses were performed on a high-performance computing cluster at Albert Einstein College of Medicine. Several quality control steps were taken to ensure accuracy of the analyzed results. Picard tools, version 1.119,<sup>16</sup> was used to demultiplex and generate FASTQ files, which were then trimmed for poor-quality bases and adaptor sequences by using Trim Galore!, version 0.3.7.<sup>17</sup> By using STAR, version 2.5.1b,<sup>18</sup> and gene annotations from Ensembl release 83,<sup>19</sup> the trimmed reads were aligned to the UCSC hg38 human genome assembly, and gene counts were generated.

Gene counts were normalized, and between-group comparison was performed with DESeq<sup>20</sup> on R statistical software, version 3.2.2. Using principal component analysis, we investigated the contribution of biological and technical covariates in the variance of normalized counts between the study groups (Fig 1). Although fasting insulin level was the only biological variable associated with variance, several technical factors, including total number of reads, protein coding reads, percentage of duplicate reads, and sequencing batch were determined to significantly contribute to the variance in the gene counts. There was no association of lipids (high-density lipoprotein, low-density lipoprotein, or triglycerides) with gene-count variance. Given the association of gene-count variance with both biological and technical factors, multivariate linear regression analysis was conducted to identify between-group differential gene expression, adjusting for the biologic and each of the technical factors. Age, sex, and ethnicity were included in the model for their demographic significance. Genes identified by means of multivariate analysis to be differentially expressed among obese asthmatic patients with a between-group *P* value of less than .05 and a false discovery rate *q*-value of less than 0.05 were retained as high confidence differentially expressed genes for verification and validation studies. The Search Tool for the Retrieval of Interacting Genes/Proteins (STRING) database, version 10,<sup>21</sup> was used to identify relationships between differentially expressed genes. Gene expression data and patients' characteristics are available at Gene Expression Omnibus number GSE86430.

**Verification and validation of directional RNA-seq results.** A subset of the high-confidence differentially expressed genes was verified by using quantitative RT-PCR (qRT-PCR) on RNA isolated from CD4<sup>+</sup> T cells from 32 children from the discovery cohort (16 children per study group). These genes and additional related genes were further validated in the validation cohort. Verification and validation was done by means of quantitative PCR by using the TaqMan gene expression assay with commercially available quantitative PCR primers (Thermo Fisher) and analyzed by using the  $\Delta\Delta$  cycle threshold method.

**Protein quantification as additional validation of differential gene expression.** CDC42EP4 and DOCK5 proteins were quantified to additionally validate differential gene expression, and phosphorylated and total p38 and S6K1 proteins were quantified as evidence for mitogen-activated protein kinase (MAPK) and mammalian target of rapamycin (mTOR) pathway activation in T-cell lysates from a subset of 5 samples from obese asthmatic patients and 4 samples from normal-weight children with asthma and normalized to actin. All antibodies, except for CDC42EP4 (Thermo Fisher Scientific), were purchased from Santa Cruz Biotechnology (Dallas, Tex). Western blot experiments were run as per protocol (Bio-Rad Laboratories, Hercules, Calif). Immunoblot band intensity was quantified with ImageJ software (National Institutes of Health, Bethesda, Md).

**Statistical analysis**

Clinical characteristics were compared between obese and normal-weight asthmatic patients by using the Student *t* test for continuous variables and the  $\chi^2$  or Fisher exact test for categorical variables. Between-group comparison of the log<sub>10</sub> transformed differential gene expression by using qRT-PCR was done with the Student *t* test. Normalized gene counts of the high-confidence differentially expressed genes were log transformed for correlation analysis with pulmonary function indices. Statistical analysis was performed on STATA software, version 14 (StataCorp, College Station, Tex).

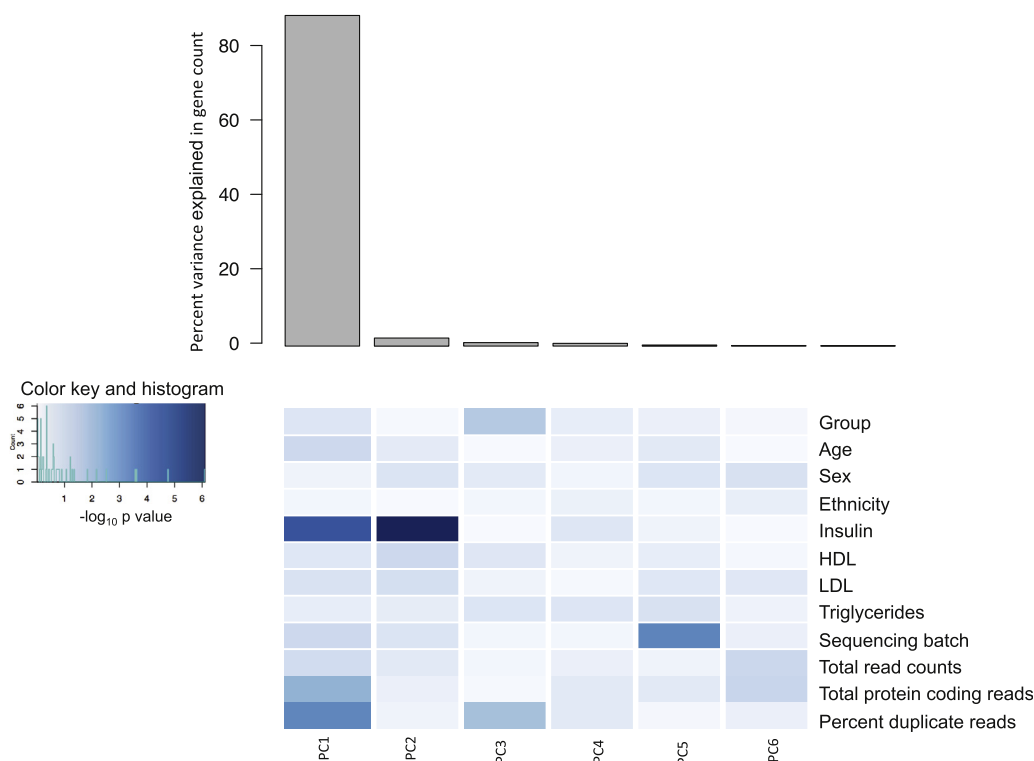


**FIG 1.** Principal component analysis of biological and technical covariates. Principal component (PC) 1 was the most important component, as seen in the bar graph. The heat map depicts the strength of the contribution of the study group and of the biologic and technical covariates on the variance of gene count for each of the top 6 principal components, highlighting the individual factors that contribute to principal component 1. The darker the intensity of blue color, the stronger the contribution of the covariate in the variance of the gene count in each principal component, as shown in the color key. *HDL*, High-density lipoprotein; *LDL*, low-density lipoprotein.

## RESULTS

### Study population

The clinical characteristics of the discovery and validation cohort are summarized in [Tables I](#) and [II](#), respectively.<sup>22</sup> Obese asthmatic children did not differ in age, sex, or ethnicity distribution from normal-weight asthmatic children in either the discovery or validation cohort. More normal-weight than obese children had evidence of atopic sensitization in the discovery cohort. In keeping with prior studies, obese children in the discovery cohort had lower percent predicted forced vital capacity (FVC), FEV<sub>1</sub>, residual volume (RV), and functional residual capacity (FRC) and RV/total lung capacity (TLC) ratio compared with normal-weight children with asthma. In the validation cohort, although RV, RV/TLC ratio, and FRC, were lower among obese children compared with normal-weight children, only FRC was significantly different between the 2 groups. Pulmonary function values were consistent between the obese asthmatic group in the 2 cohorts, other than percent predicted RV, but there was greater variability in FVC, FEV<sub>1</sub>, and RV/TLC ratio between the 2 normal-weight groups.

### Analysis and validation of differential CD4<sup>+</sup> T-cell gene expression

Univariate analysis by using DESeq revealed differential gene expression of 1371 genes in CD4<sup>+</sup> T cells from obese asthmatic

compared with normal-weight patients, with more genes being upregulated in the obese compared with normal-weight asthmatic patients ([Fig 2, A](#)). After adjusting in multivariate regression analysis for the biological and technical factors associated with gene-count variance, 319 genes were differentially expressed among obese compared with normal-weight asthmatic children (between-group  $P < .05$ ,  $q\text{-value} < 0.05$ ; [Fig 2, B](#), and see [Table E1](#) in this article's Online Repository at [www.jacionline.org](http://www.jacionline.org)). Of these, 89 genes overlapped between the initial DESeq analysis and multivariate analysis (see [Table E2](#) in this article's Online Repository at [www.jacionline.org](http://www.jacionline.org)).

Gene network analysis of these 89 genes revealed CDC42 to be at the hub of the differentially expressed genes ([Fig 3](#)). Moreover, 24 of the 89 upregulated genes among obese asthmatic patients were associated with modulation of the small guanosine triphosphate (GTP)-binding proteins CDC42 and RAC1 ([Table III](#)). Of particular relevance were VAV2, DOCK5, PAK3, PLD1, CDC42BPB, and CDC42EP4, which either interact directly with the CDC42 protein (CDC42EP4), are upstream modulators (VAV2 and DOCK5), or are downstream targets of CDC42 (PAK3, PLD1, and CDC42BPB). We verified the expression of CDC42EP4 because it directly interacts with CDC42, and DOCK5 and VAV2, its upstream modulators, using qRT-PCR ([Fig 4](#)). Although expression of CDC42EP4 and DOCK5 was significantly higher among obese asthmatic patients, there was a nonsignificant trend of higher VAV2 expression in obese asthmatic patients ([Fig 4](#) and see [Fig E2](#) in this article's Online Repository at

**TABLE I.** Demographic and clinical characteristics of the discovery cohort

	Obese asthmatic patients (n = 21)	Normal-weight asthmatic patients (n = 21)	P value
Age (y)	9.1 ± 1.5	8.9 ± 0.6	.76
Male sex, no. (%)	8 (38.1)	10 (47.6)	.75
Hispanic, no. (%)	15 (71.4)	12 (57.4)	.52
BMI z score	1.9 ± 0.4	0.06 ± 0.8	<.001
Atopic sensitization*	17 (81)	20 (95.2)	.01
Insulin	11.9 ± 7.5	8.5 ± 4.7	.08
FVC†	102 ± 11.1	89.7 ± 12.3	.002
FEV <sub>1</sub> †	96.2 ± 16.7	87.1 ± 16.4	.08
FEV <sub>1</sub> /FVC	81.7 ± 7.5	84.5 ± 8.4	.27
TLC†	92.6 ± 13.5	92 ± 11	.88
RV†	86.6 ± 36.2	120.4 ± 33.7	.004
RV/TLC†	22 ± 6.2	31.8 ± 6	<.001
ERV†	77.2 ± 17.7	81.1 ± 29.7	.62
FRC†	85.3 ± 19.4	105.8 ± 23.4	.005
Medication use			
Inhaled steroids	11 (52.3)	9 (42.9)	.75
Montelukast	13 (61.9)	9 (42.9)	.35
Inhaled steroid/long-acting β-agonist combination therapy	3 (14.3)	4 (19)	1

All continuous variables are reported as means ± SDs. Categorical variables (sex [male] and ethnicity [Hispanic]), atopic sensitization, and medication use are reported as group-specific numeric frequencies and percentages.

BMI, Body mass index; ERV, expiratory reserve volume.

\*Atopic sensitization was defined as skin prick test reactivity to 1 or more allergens.<sup>22</sup>

†Pulmonary function variables are reported as percent predicted values, other than FEV<sub>1</sub>/FVC and RV/TLC ratio, which are reported as percentages.

**TABLE II.** Demographic and clinical characteristics of the validation cohort

	Obese asthmatic patients (n = 10)	Normal-weight asthmatic patients (n = 10)	P value
Age (y)	8.8 ± 1	8.6 ± 1.4	.71
Male sex, no. (%)	5 (50)	8 (80)	.34
Hispanic, no. (%)	5 (50)	5 (50)	1
BMI z score	1.8 ± 0.5	0.1 ± 1.01	<.001
Atopic sensitization*	8 (80)	8 (80)	1
Insulin	13.9 ± 5.8	12.2 ± 6.2	.6
FVC†	102 ± 14	105 ± 22	.76
FEV <sub>1</sub> †	91.5 ± 19	100.1 ± 21	.36
FEV <sub>1</sub> /FVC	77.1 ± 8	82.9 ± 4	.08
TLC†	94.4 ± 10	98 ± 14	.54
RV†	100.4 ± 32	110.1 ± 22	.43
RV/TLC	25.6 ± 7	27.9 ± 4	.39
ERV†	71.1 ± 24	99.8 ± 25	.02
FRC†	90.1 ± 18	112.2 ± 17	.02
Medication use			
Inhaled steroids	5 (50)	5 (50)	1
Montelukast	9 (90)	7 (70)	.58
Inhaled steroid/long-acting β-agonist combination therapy	4 (40)	2 (20)	.62

All continuous variables are reported as means ± SDs. Categorical variables (sex [male] and ethnicity [Hispanic]), atopic sensitization, and medication use are reported as group-specific numerical frequency and percentages.

BMI, Body mass index; ERV, expiratory reserve volume.

\*Atopic sensitization was defined as skin prick test reactivity to 1 or more allergens.

†Pulmonary function variables are reported as percent predicted values, other than FEV<sub>1</sub>/FVC and RV/TLC ratio, which are reported as percentages.

[www.jacionline.org](http://www.jacionline.org)). Because several differentially expressed genes were associated with both CDC42 and RAC1 activation, we quantified RAC1 expression and found no differential expression (Fig 4). Therefore we focused on validating these differentially expressed genes and additional downstream genes (PAK3, PLD1, MLK3, and cRaf1) in the validation cohort (Fig 5) as confirmation of upregulation of the CDC42 pathway in obese asthmatic CD4<sup>+</sup> T cells. Although MLK3, PAK3, and PLD1

were upregulated in obese asthmatic patients, cRaf1 was not differentially expressed (Fig 5).

Immunoblot analysis was done to confirm that higher mRNA expression of CDC42EP4 and DOCK5 translated into higher protein expression. In keeping with the RNA-Seq and quantitative PCR data, we found a trend toward higher levels of these 2 proteins, although the trend did not reach statistical significance (see Fig E3 in this article's Online Repository at



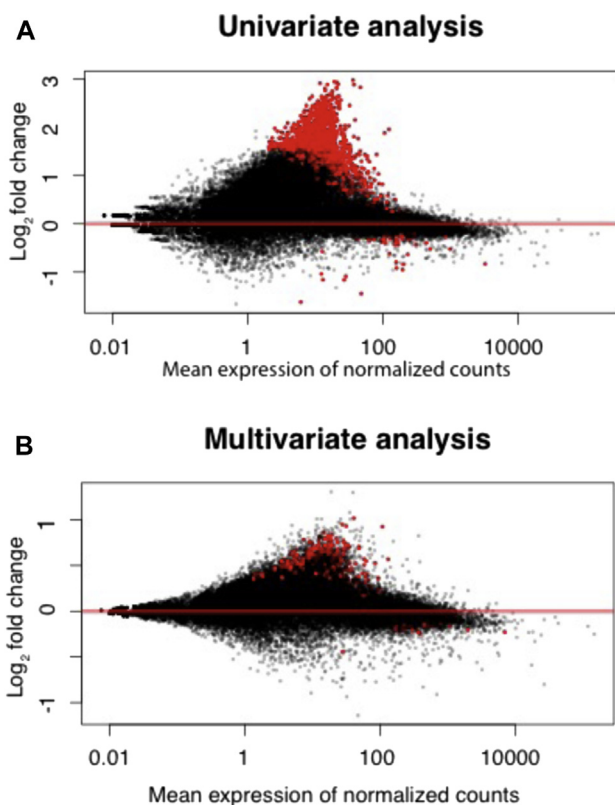


**FIG 2.** MA plot of fold change and mean gene expression by using DESeq analysis before adjustment for biological and technical covariates (univariate analysis; **A**) and after adjustment for biological and technical covariates (multivariate analysis; **B**). Red dots denote differentially expressed genes among obese asthmatic patients at a false discovery rate  $q$ -value of less than 0.05.

[www.jacionline.org](http://www.jacionline.org)). Similarly, there was a nonsignificant trend toward higher levels of S6K1 phosphorylation in T cells from obese asthmatic patients, which was supportive of activation of the CDC42-mTOR signaling pathway.

To elucidate clinical significance, we correlated gene transcript counts with pulmonary function variables. We found an inverse association between log-transformed normalized gene counts of *CDC42EP4* and *DOCK5* and FEV<sub>1</sub>/FVC ratios only among obese asthmatic patients (Fig 6), ascribing clinical relevance to the differential gene expression.

## DISCUSSION

Our study provides novel evidence that the transcriptome of CD4<sup>+</sup> T cells derived from obese asthmatic children differs from that of CD4<sup>+</sup> T cells from children with normal-weight asthma. Specifically, we found that several genes associated with the small GTP-binding protein CDC42 were upregulated in T cells from obese children with asthma. Although VAV2 and *DOCK5* are upstream of and activate CDC42, *CDC42EP4* interacts directly with CDC42, and *CDC2BPB*, *PAK3*, and *PLD1* are downstream effectors, mediating the different effects of this ubiquitous GTP protein. Furthermore, *CDC42EP4* and *DOCK5* gene transcript counts correlated with lower airway obstruction, suggesting that the CDC42 pathway might have clinical implications in pediatric obesity-related asthma.

Few of these genes have been previously studied in the context of inflammation in asthma or obesity.<sup>23</sup> However, the role of CDC42 and its related proteins has been researched extensively in the context of T-cell physiology. VAV2 and *DOCK5*, which are upregulated in T cells from obese asthmatic patients, are guanine exchange factors that activate CDC42.<sup>24</sup> VAV2 is ubiquitously expressed and associated with activation of CDC42<sup>25</sup> and its downstream c-JUN transcription factor,<sup>25</sup> leading to CDC42-mediated activation of the MAP kinase pathway.<sup>26</sup> DOCK proteins are less well studied in T cells. Although *DOCK5*, a member of DOCK family A,<sup>27</sup> is classically associated with activation of RAC1,<sup>28</sup> it influences the degranulation response in mast cells through the NCK-AKT pathway independent of the RAC1 activation,<sup>29</sup> suggesting that it might have additional effects on immune cells. Because our study is the first to identify upregulation of *DOCK5* and its association with CDC42 in T cells, further investigation of its effects and related downstream molecules are needed to identify its role in T cells.

We also confirmed upregulation of downstream targets of CDC42, including *PAK3*, *MLK3*, and *PLD1* but not cRaf1. *PAK3*, with CDC42, plays a role in immunologic synapse formation<sup>30–32</sup> and is associated with activation of MAPK and mTOR immune pathways.<sup>33–35</sup> Higher *MLK3* expression also supports downstream activation of the MAPK pathway as a potential mechanism underlying T<sub>H</sub>1 polarization among obese asthmatic children. Similarly, *PLD1* activation by CDC42<sup>36</sup> mediates S6K1 activation in the mTOR pathway,<sup>34</sup> which regulates T<sub>H</sub>1 and T<sub>H</sub>17 differentiation.<sup>37</sup> Quantified in resting cells, we found a small nonsignificant trend for higher phosphorylated S6K1 levels in T cells from obese asthmatic patients. Together, upregulated gene expression of upstream guanine exchange factors and downstream effectors provide evidence of activation of CDC42-related pathways that have been associated with T<sub>H</sub> cell activation and might explain the differentiation bias toward a T<sub>H</sub>1 lineage,<sup>37</sup> a phenotype observed among obese asthmatic children.<sup>6,11</sup> Moreover, the inverse association of *CDC42EP4* and *DOCK5* gene counts with FEV<sub>1</sub>/FVC ratio uniquely in obese asthmatic patients provides additional evidence of its relevance in the obese asthma phenotype.

In light of the association of nonatopic systemic inflammation with disease burden in obese asthmatic adults<sup>38</sup> and children,<sup>6,11</sup> we speculate that CDC42 activation in T cells from obese asthmatic patients might play several roles, including skewing of T-cell differentiation to a T<sub>H</sub>1/T<sub>H</sub>17 profile, increased T-cell tissue recruitment by facilitating transmigration, and T-cell activation. Because these pathways are distinct from those activated in patients with atopic asthma,<sup>39</sup> our findings begin to identify immune pathways associated with nonatopic immune responses in patients with the obese asthma phenotype. Activation of Rho GTPases, including CDC42, has been proposed to underlie T-cell activation in patients with T<sub>H</sub>1-mediated autoimmune diseases, such as lupus.<sup>40</sup> Validation of our findings would support potential extension of therapeutics used for autoimmune diseases to obesity-related asthma. Although the direct mechanism by which circulating T cells influence pulmonary physiology in obese patients with asthma is not known at this time, we hypothesize that T cells might increase neutrophilic airway inflammation<sup>41</sup> or influence airway smooth muscle contractility and proliferation,<sup>42</sup> mechanisms that have been proposed to underlie the obese asthma phenotype and warrant further investigation.

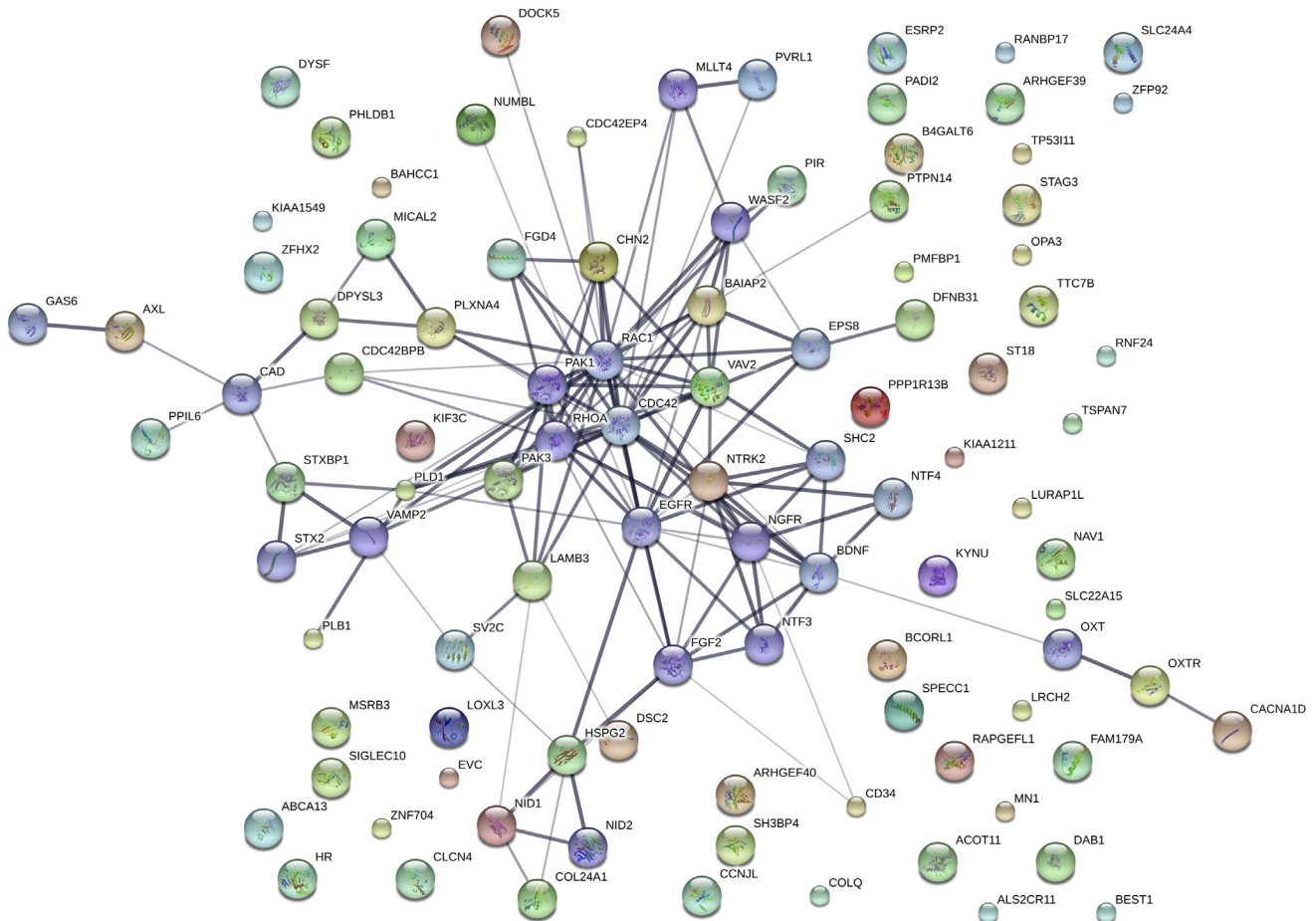


**FIG 3.** Association between differentially expressed high-confidence genes. The thickness of the connecting lines reflects the strength of the association.

We have previously reported an association between insulin resistance and systemic  $T_H1$  polarization in urban minority children.<sup>11</sup> In the current study insulin was significantly associated with gene-count variance. T-cell activation is associated with aerobic glycolysis,<sup>43</sup> increased cellular glucose uptake caused by translocation of glucose transporter 1 (GLUT1),<sup>44</sup> and *de novo* expression of the insulin receptor on the cell surface,<sup>45</sup> suggesting a metabolic role for insulin in T-cell activation. Because the insulin signaling pathway uses CDC42 for glucose transport in adipocytes,<sup>46</sup> we hypothesize that the same mechanism can be used to address the activated T cell's increased glucose needs.<sup>43</sup> Thus upregulation of the CDC42 pathway identifies a need for further exploration of these immunometabolic pathways in patients with chronic diseases, such as obesity-related asthma.

Our study has several strengths. It is the first study to investigate the  $T_H$  cell transcriptome using directional RNA-seq and identifies the CDC42 pathway as a key upregulated pathway in obese asthmatic children that is associated with lower airway obstruction. The  $T_H$  cell transcriptomic findings were validated in a separate cohort of 10 obese and 10 normal-weight children with asthma. We also identified the influence of technical and biological covariates on differential gene expression in a disease state, highlighting the importance of addressing these to allow for the identification of high confidence genes. These findings

in negatively selected unstimulated T cells unmodified by any external mitogenic influences are more reflective of *in vivo* responses and are novel because prior studies of unstimulated T cell transcriptome did not find differences between cases and control subjects.<sup>47</sup> However, there are certain limitations. Asthma diagnosis in our cohort was based on physician diagnosis rather than objective assessment of airway reactivity. We found small fold differences in the gene expression and nonsignificant differences in the corresponding and downstream proteins. Because these cells were derived from obese children with well-controlled asthma in the absence of a recent exacerbation, it is unlikely that the cells would be markedly activated with increased protein levels, as can be observed in the setting of an asthma exacerbation. Furthermore, the lack of an obese nonasthmatic control group limited the understanding of the extent to which differential gene expression was driven by obesity alone. In addition, our study is cross-sectional in nature, and therefore a cause-effect relationship could not be derived. Nonetheless, the upregulation of several genes associated with the CDC42 pathway upstream of both the MAPK and mTOR pathways suggests that these pathways might be poised for activation in the setting of poor disease control or an exacerbation and thereby provides direction for further investigation to identify the key molecules that might be associated with nonatopic  $T_H1$  systemic inflammation in patients with obesity-related asthma.

**TABLE III.** Genes associated with activation of the small GTP proteins CDC42 and RAC1

Ensembl ID	Associated gene name	Log <sub>2</sub> fold change	q-value
ENSG00000168453	<i>HR</i>	2.599971402	2.32E-05
ENSG00000204764	<i>RANBP17</i>	2.251636516	0.000253142
ENSG00000157388	<i>CACNA1D</i>	1.8684354	0.002357941
ENSG00000137135	<i>ARHGEF39</i>	1.850566818	0.001725958
ENSG00000115318	<i>LOXL3</i>	1.663949396	0.015247401
ENSG00000163803	<i>PLB1</i>	1.649412493	0.0013521
ENSG00000087842	<i>PIR</i>	1.61362157	0.020860028
ENSG00000173406	<i>DAB1</i>	1.553990563	0.016608231
ENSG00000139132	<i>FGD4</i>	1.453418533	0.008949179
ENSG00000075651	<i>PLD1</i>	1.361719192	0.018931263
ENSG00000160293	<i>VAV2</i>	1.332433107	0.012568743
ENSG00000130147	<i>SH3BP4</i>	1.310248419	0.031128422
ENSG00000142512	<i>SIGLEC10</i>	1.290791208	0.030722074
ENSG00000165801	<i>ARHGEF40</i>	1.285779282	0.034584495
ENSG00000105245	<i>NUMBL</i>	1.242714423	0.014961879
ENSG00000106069	<i>CHN2</i>	1.220243828	0.018341102
ENSG00000167601	<i>AXL</i>	1.216368793	0.049907113
ENSG00000175866	<i>BAIAP2</i>	1.125602885	0.021294253
ENSG00000147459	<i>DOCK5</i>	1.101075872	0.03490964
ENSG00000198752	<i>CDC42BPB</i>	0.87291003	0.022874905
ENSG00000088808	<i>PPP1R13B</i>	0.642280439	0.020469995
ENSG00000101236	<i>RNF24</i>	0.572603051	0.028734724
ENSG00000077264	<i>PAK3</i>	0.538432709	0.0141306

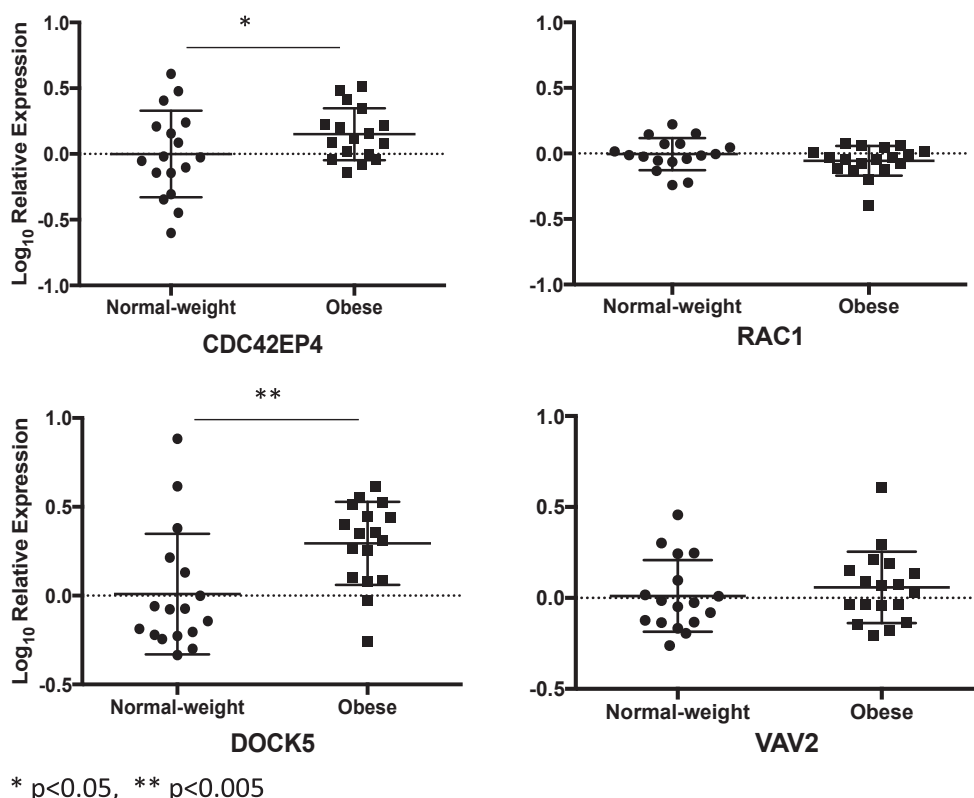


**FIG 4.** Verification of a subset of genes in the first cohort of samples by using qRT-PCR. Log<sub>10</sub> fold differential gene expression is compared between obese and normal-weight children with asthma.

In summary, we found upregulation of several genes associated with the small GTP protein CDC42, which is involved in many T-cell functions, including antigen recognition through the

immunologic synapse, intracellular transport and vesicle formation for cytokine release, and T-cell activation with activation of the MAPK and mTOR pathways. These genes and their

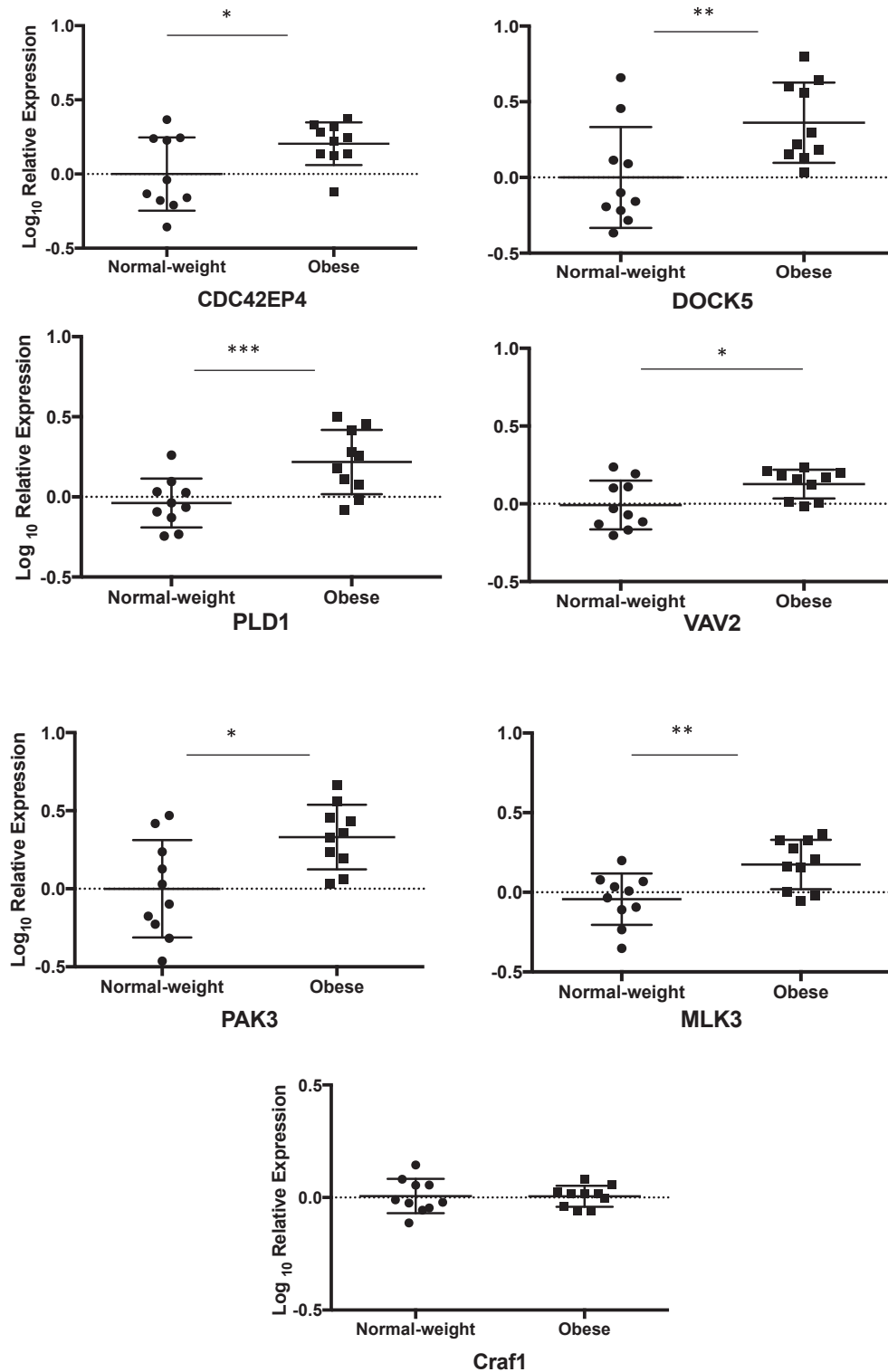


**FIG 5.** Validation of the subset of genes in the second cohort of samples by using qRT-PCR.  $\text{Log}_{10}$  fold differential gene expression was compared between  $T_H$  cells from obese asthmatic and those from normal-weight asthmatic patients. In addition to genes investigated in the verification experiment (Fig 4), differential expression of additional genes downstream of CDC42, including MLK3 and cRAF1, were investigated. Although expression of MLK3 was higher in  $T_H$  cells from obese asthmatic patients, that of cRAF1 did not differ between  $T_H$  cells from obese and those from normal-weight asthmatic patients. \* $P < .05$ , \*\* $P < .01$ , and \*\*\* $P < .005$ .



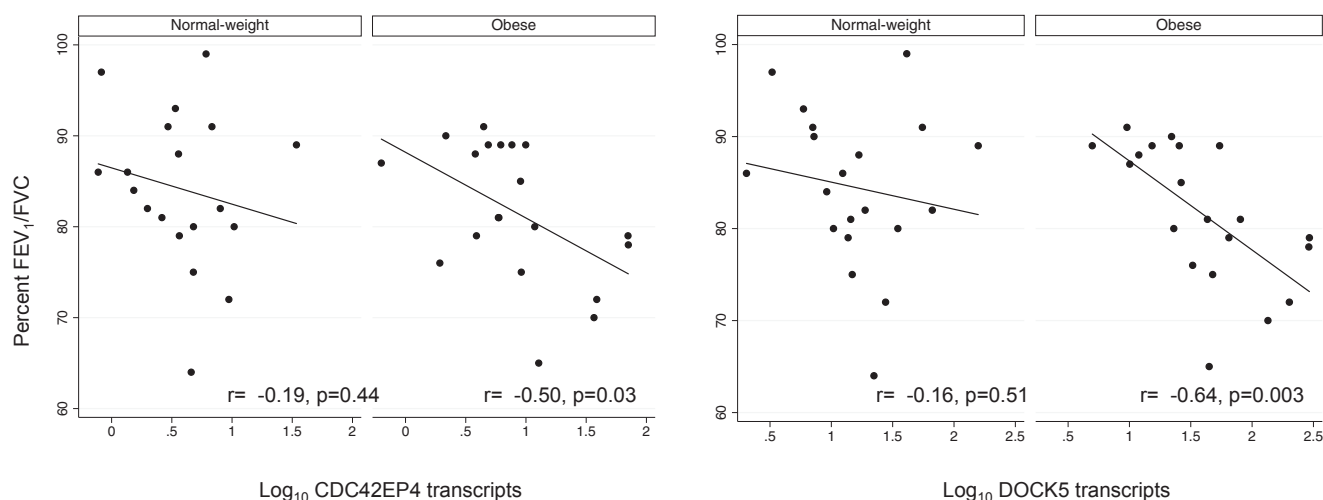


**FIG 6.** Association of *CDC42EP4* and *DOCK5* gene counts with FEV<sub>1</sub>/FVC ratio. Log<sub>10</sub> transformed *CDC42EP4* and *DOCK5* gene counts were inversely correlated with FEV<sub>1</sub>/FVC ratio only in obese asthmatic children.

associated pathways provide direction for further investigation of key regulatory molecules underlying the nonatopic T-cell inflammation in obese asthmatic patients that can serve as therapeutic targets for pediatric obesity-related asthma.

We thank all the participating children and their families for taking the time to complete the study protocol. We also acknowledge the staff at the Epigenomics Shared Facility and the High-Performance Computing Core Facility at Albert Einstein College of Medicine for the sequencing and post sequencing processing of the RNA-Seq experiments.

### Key messages

- T<sub>H</sub> cells from obese asthmatic children have a distinct transcriptome when compared with T<sub>H</sub> cells from normal-weight children.
- Expression of genes related to CDC42, a GTP protein, which plays a role in T-cell activation, was upregulated in T<sub>H</sub> cells from obese asthmatic children.
- Expression of *MLK3* and *PLDI*, genes downstream of CDC42 in the MAPK and mTOR pathways, respectively, was upregulated in T<sub>H</sub> cells from obese asthmatic patients, suggesting that pathways activated distal to CDC42 might play a role in the non-atopic T<sub>H</sub>1 immune responses previously observed in obese asthmatic children.
- Transcript abundance of genes in the CDC42 pathway directly correlated with lower airway obstruction in obese asthmatic children.

### REFERENCES

1. Ogden CL, Carroll MD, Kit BK, Flegal KM. Prevalence of obesity and trends in body mass index among US children and adolescents, 1999-2010. *JAMA* 2012; 307:483-90.
2. Akinbami LJ, Simon AE, Rossen LM. Changing trends in asthma prevalence among children. *Pediatrics* 2016;137.
3. Chen YC, Dong GH, Lin KC, Lee YL. Gender difference of childhood overweight and obesity in predicting the risk of incident asthma: a systematic review and meta-analysis. *Obes Rev* 2013;14:222-31.
4. Wenzel SE. Asthma phenotypes: the evolution from clinical to molecular approaches. *Nat Med* 2012;18:716-25.
5. Lang JE, Hossain J, Smith K, Lima JJ. Asthma severity, exacerbation risk, and controller treatment burden in underweight and obese children. *J Asthma* 2012; 49:456-63.
6. Rastogi D, Canfield S, Andrade A, Hall CB, Isasi CR, Rubinstein A, et al. Obesity-associated asthma in children: a distinct entity. *Chest* 2012;141:895-905.
7. McGarry ME, Castellanos E, Thakur N, Oh SS, Eng C, Davis A, et al. Obesity and bronchodilator response in black and Hispanic children and adolescents with asthma. *Chest* 2015;147:1591-8.
8. Chen Y, Rennie D, Cormier Y, Dosman JA. Waist circumference associated with pulmonary function in children. *Pediatr Pulmonol* 2009;44:216-21.
9. Arshi M, Cardinal J, Hill RJ, Davies PS, Wainwright C. Asthma and insulin resistance in children. *Respirology* 2010;15:779-84.
10. Cottrell L, Neal WA, Ice C, Perez MK, Piedimonte G. Metabolic abnormalities in children with asthma. *Am J Respir Crit Care Med* 2011;183:441-8.
11. Rastogi D, Fraser S, Oh J, Huber AM, Schulman Y, Bhagani RH, et al. Inflammation, metabolic dysregulation and pulmonary function among obese asthmatic urban adolescents. *Am J Resp Crit Care Med* 2015;191:149-60.
12. Guilbert TW, Mauger DT, Lemanske RF Jr. Childhood asthma-predictive phenotype. *J Allergy Clin Immunol Pract* 2014;2:664-70.
13. Georas SN, Guo J, De Fanis U, Casolaro V. T-helper cell type-2 regulation in allergic disease. *Eur Respir J* 2005;26:1119-37.
14. Busse WW, Morgan WJ, Gergen PJ, Mitchell HE, Gern JE, Liu AH, et al. Randomized trial of omalizumab (anti-IgE) for asthma in inner-city children. *N Engl J Med* 2011;364:1005-15.
15. Podnar J, Deiderick H, Huerta G, Hunnicke-Smith S. Next-generation sequencing RNA-Seq library construction. *Curr Protoc Mol Biol* 2014;106:1-19.
16. Available at: <http://broadinstitute.github.io/picard/>. Accessed February 25, 2016.
17. Available at: [http://www.bioinformatics.babraham.ac.uk/projects/trim\\_galore/](http://www.bioinformatics.babraham.ac.uk/projects/trim_galore/). Accessed February 25, 2016.
18. Dobin A, Davis CA, Schlesinger F, Drenkow J, Zaleski C, Jha S, et al. STAR: ultrafast universal RNA-Seq aligner. *Bioinformatics* 2013;29:15-21.
19. Flicek P, Amode MR, Barrell D, Beal K, Billis K, Brent S, et al. Ensembl 2014. *Nucleic Acids Res* 2014;42(Database issue):D749-55.
20. Anders S, Huber W. Differential expression analysis for sequence count data. *Genome Biol* 2010;11:R106.
21. Szklarczyk D, Franceschini A, Wyder S, Forslund K, Heller D, Huerta-Cepas J, et al. STRING v10: protein-protein interaction networks, integrated over the tree of life. *Nucleic Acids Res* 2015;43(Database issue):D447-52.
22. Salo PM, Arbes SJ Jr, Jaramillo R, Calatroni A, Weir CH, Sever ML, et al. Prevalence of allergic sensitization in the United States: results from the National Health and Nutrition Examination Survey (NHANES) 2005-2006. *J Allergy Clin Immunol* 2014;134:350-9.
23. Lee SM, Choi HJ, Oh CH, Oh JW, Han JS. Leptin increases TNF- $\alpha$  expression and production through phospholipase D1 in Raw 264.7 cells. *PLoS One* 2014;9:e102373.
24. Liu BP, Burrridge K. Vav2 activates Rac1, Cdc42, and RhoA downstream from growth factor receptors but not beta1 integrins. *Mol Cell Biol* 2000;20:7160-9.

25. Abe K, Rossman KL, Liu B, Ritola KD, Chiang D, Campbell SL, et al. Vav2 is an activator of Cdc42, Rac1, and RhoA. *J Biol Chem* 2000;275:10141-9.
26. Kyriakis JM, Avruch J. Mammalian MAPK signal transduction pathways activated by stress and inflammation: a 10-year update. *Physiol Rev* 2012;92:689-737.
27. Namekata K, Kimura A, Kawamura K, Harada C, Harada T. Dock GEFs and their therapeutic potential: neuroprotection and axon regeneration. *Prog Retin Eye Res* 2014;43:1-16.
28. Watanabe M, Terasawa M, Miyano K, Yanagihara T, Uruno T, Sanematsu F, et al. DOCK2 and DOCK5 act additively in neutrophils to regulate chemotaxis, superoxide production, and extracellular trap formation. *J Immunol* 2014;193:5660-7.
29. Ogawa K, Tanaka Y, Uruno T, Duan X, Harada Y, Sanematsu F, et al. DOCK5 functions as a key signaling adaptor that links FcεRI signals to microtubule dynamics during mast cell degranulation. *J Exp Med* 2014;211:1407-19.
30. Salazar-Fontana LI, Barr V, Samelson LE, Bierer BE. CD28 engagement promotes actin polymerization through the activation of the small Rho GTPase Cdc42 in human T cells. *J Immunol* 2003;171:2225-32.
31. Vicente-Manzanares M, Sánchez-Madrid F. Role of the cytoskeleton during leukocyte responses. *Nat Rev Immunol* 2004;4:110-22.
32. Tskvitaria-Fuller I, Seth A, Mistry N, Gu H, Rosen MK, Wülfing C. Specific patterns of Cdc42 activity are related to distinct elements of T cell polarization. *J Immunol* 2006;177:1708-20.
33. Zhong B, Jiang K, Gilvary DL, Epling-Burnette PK, Ritchey C, Liu J, et al. Human neutrophils utilize a Rac/Cdc42-dependent MAPK pathway to direct intracellular granule mobilization toward ingested microbial pathogens. *Blood* 2003;101:3240-8.
34. Fang Y, Park IH, Wu AL, Du G, Huang P, Frohman MA, et al. PLD1 regulates mTOR signaling and mediates Cdc42 activation of S6K1. *Curr Biol* 2003;13:2037-44.
35. Kaga S, Ragg S, Rogers KA, Ochi A. Activation of p21-CDC42/Rac-activated kinases by CD28 signaling: p21-activated kinase (PAK) and MEK kinase 1 (MEKK1) may mediate the interplay between CD3 and CD28 signals. *J Immunol* 1998;160:4182-9.
36. Henage LG, Exton JH, Brown HA. Kinetic analysis of a mammalian phospholipase D: allosteric modulation by monomeric GTPases, protein kinase C, and polyphosphoinositides. *J Biol Chem* 2006;281:3408-17.
37. Delgoffe GM, Polizzi KN, Waickman AT, Heikamp E, Meyers DJ, Horton MR, et al. The kinase mTOR regulates the differentiation of helper T cells through the selective activation of signaling by mTORC1 and mTORC2. *Nat Immunol* 2011;12:295-303.
38. Peters MC, McGrath KW, Hawkins GA, Hastie AT, Levy BD, Israel E, et al. Plasma interleukin-6 concentrations, metabolic dysfunction, and asthma severity: a cross-sectional analysis of two cohorts. *Lancet Respir Med* 2016;4:574-84.
39. Holt PG, Sly PD. Interaction between adaptive and innate immune pathways in the pathogenesis of atopic asthma: operation of a lung/bone marrow axis. *Chest* 2011;139:1165-71.
40. Pernis A. Rho GTPase-mediated pathways in mature CD4+ T cells. *Autoimmun Rev* 2009;9:199-203.
41. Scott HA, Gibson PG, Garg ML, Upham JW, Wood LG. Sex hormones and systemic inflammation are modulators of the obese-asthma phenotype. *Allergy* 2016;71:1037-47.
42. Ramos-Barbón D, Fraga-Iriso R, Brienza NS, Montero-Martínez C, Vereza-Hernando H, Olivenstein R, et al. T Cells localize with proliferating smooth muscle alpha-actin+ cell compartments in asthma. *Am J Respir Crit Care Med* 2010;182:317-24.
43. Wang R, Dillon CP, Shi LZ, Milasta S, Carter R, Finkelstein D, et al. The transcription factor Myc controls metabolic reprogramming upon T lymphocyte activation. *Immunity* 2011;35:871-82.
44. Macintyre AN, Gerriets VA, Nichols AG, Michalek RD, Rudolph MC, Deoliveira D, et al. The glucose transporter Glut1 is selectively essential for CD4 T cell activation and effector function. *Cell Metab* 2014;20:61-72.
45. Stentz FB, Kitabchi AE. Hyperglycemia-induced activation of human T-lymphocytes with de novo emergence of insulin receptors and generation of reactive oxygen species. *Biochem Biophys Res Commun* 2005;335:491-5.
46. Usui I, Imamura T, Huang J, Satoh H, Olefsky JM. Cdc42 is a Rho GTPase family member that can mediate insulin signaling to glucose transport in 3T3-L1 adipocytes. *J Biol Chem* 2003;278:13765-74.
47. Quinn EM, Coleman C, Molloy B, Dominguez Castro P, Cormican P, Trimble V, et al. Transcriptome analysis of CD4+ T cells in coeliac disease reveals imprint of BACH2 and IFNγ regulation. *PLoS One* 2015;10:e0140049.

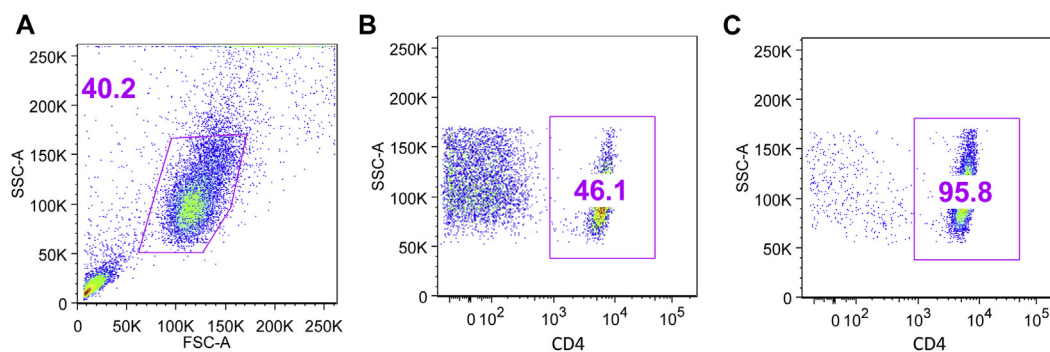


**FIG E1.** Flow cytometry–based quantification of T-cell purity after cell separation. **A**, Lymphocytes were gated based on forward scatter (FSC) and side scatter (SSC). **B** and **C**, Proportions of CD4<sup>+</sup> lymphocytes were quantified based on staining with anti-human CD4-allophycocyanin H7 antibody in freshly separated PBMCs (Fig E1, *B*) and T cells isolated by means of negative selection (Fig E1, *C*).

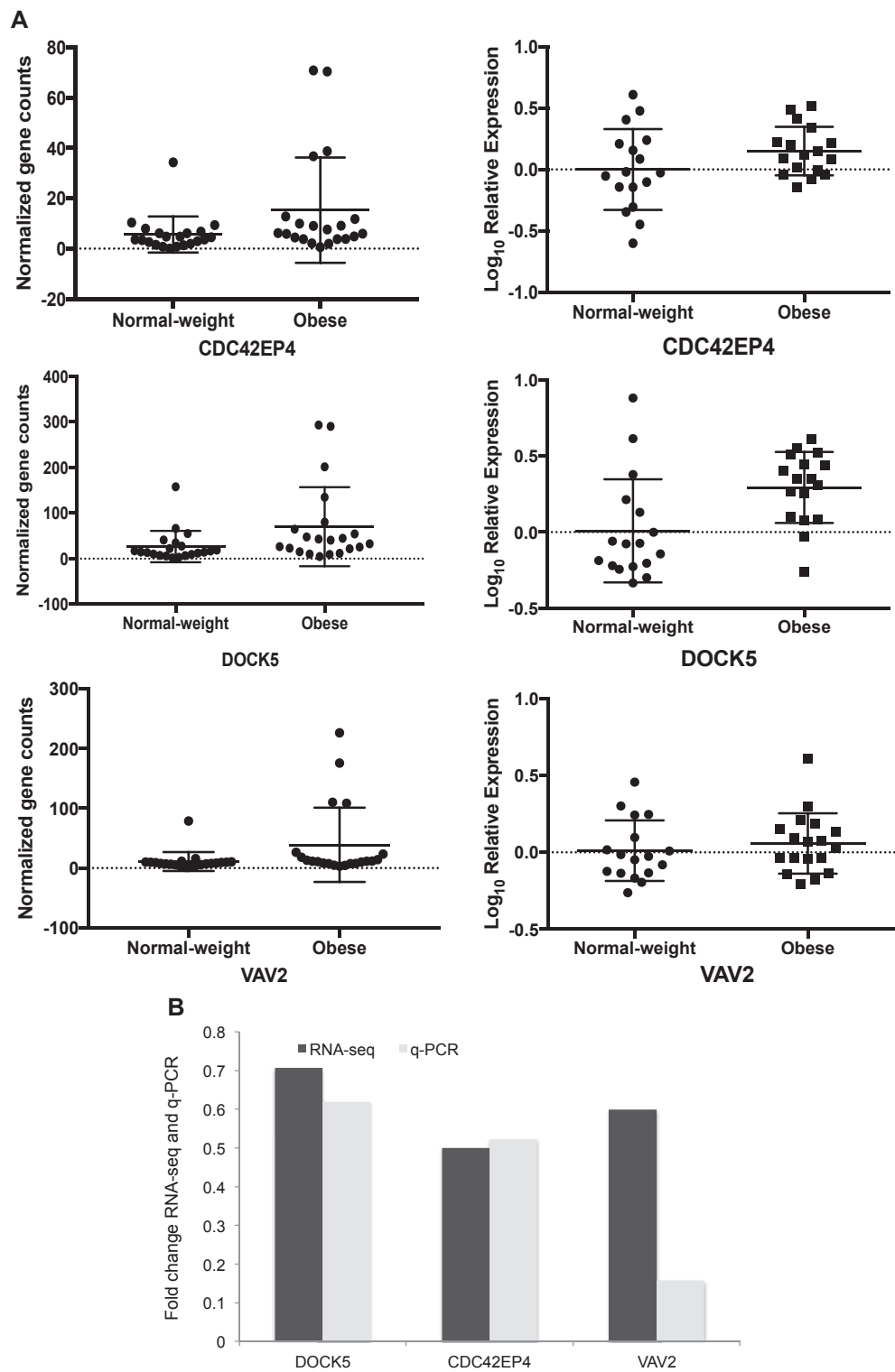


**FIG E2. A,** Visual depiction of normalized gene counts of high-confidence genes with their corresponding qRT-PCR results. **B,** Fold changes in *CDC42EP4*, *DOCK5*, and *VAV2* trended in the same direction.

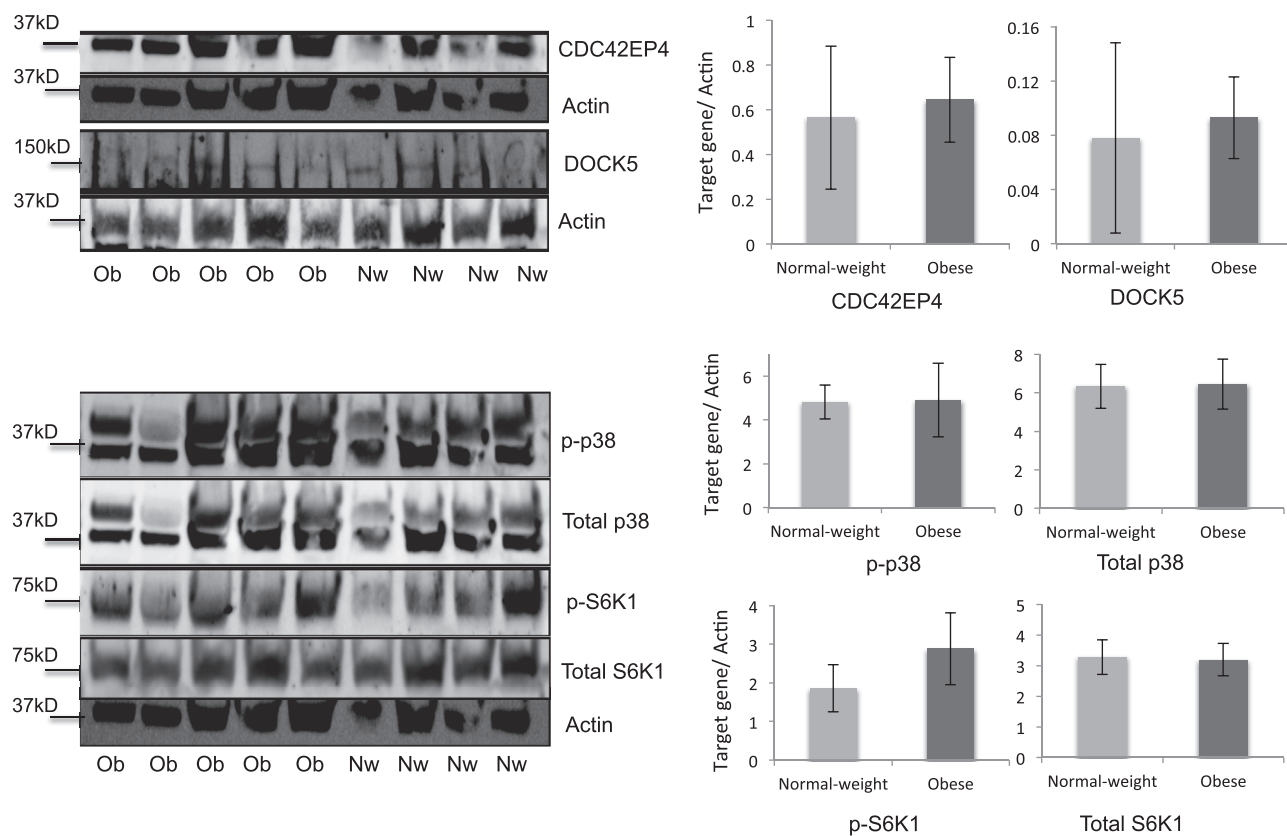


**FIG E3.** Western blot analysis of proteins corresponding to upregulated high-confidence genes and those in downstream MAPK and mTOR pathways. CDC42PE4 and DOCK5 trended toward higher levels in obese asthmatic samples. Similarly, p-S6K1 levels trended toward higher in obese asthmatic patients. However, none of these differences reached statistical significance.



**TABLE E1.** Differentially expressed genes identified by means of multivariate analysis

Ensembl ID	Associated gene name	Log <sub>2</sub> fold change	q-value
ENSG00000165914	<i>TTC7B</i>	2.764	0.001
ENSG00000135636	<i>DYSF</i>	2.579	0.004
ENSG00000179869	<i>ABCA13</i>	2.537	0.010
ENSG00000280156	<i>AC006548.28</i>	2.520	0.036
ENSG00000116962	<i>NID1</i>	2.370	0.003
ENSG00000136367	<i>ZFH2</i>	2.308	0.010
ENSG00000157110	<i>RBPMS</i>	2.288	0.008
ENSG00000092758	<i>COL9A3</i>	2.241	0.005
ENSG00000117115	<i>PADI2</i>	2.241	0.002
ENSG00000113657	<i>DPYSL3</i>	2.225	0.010
ENSG00000125046	<i>SSUH2</i>	2.222	0.011
ENSG00000175029	<i>CTBP2</i>	2.220	0.003
ENSG00000174099	<i>MSRB3</i>	2.218	0.001
ENSG00000234456	<i>MAGI2-AS3</i>	2.204	0.005
ENSG00000073464	<i>CLCN4</i>	2.187	0.001
ENSG00000174059	<i>CD34</i>	2.169	0.002
ENSG00000152104	<i>PTPN14</i>	2.156	0.014
ENSG00000155754	<i>ALS2CR11</i>	2.144	0.007
ENSG00000066056	<i>TIE1</i>	2.142	0.014
ENSG00000131398	<i>KCNC3</i>	2.128	0.005
ENSG00000168453	<i>HR</i>	2.120	0.013
ENSG00000137474	<i>MYO7A</i>	2.098	0.018
ENSG00000136854	<i>STXBP1</i>	2.093	0.001
ENSG00000176046	<i>NUPR1</i>	2.091	0.010
ENSG00000019505	<i>SYT13</i>	2.080	0.013
ENSG00000148053	<i>NTRK2</i>	2.071	0.030
ENSG00000204764	<i>RANBP17</i>	2.069	0.020
ENSG00000112414	<i>ADGRG6</i>	2.056	0.006
ENSG00000196878	<i>LAMB3</i>	2.050	0.010
ENSG00000198753	<i>PLXNB3</i>	2.034	0.017
ENSG00000137135	<i>ARHGEF39</i>	2.033	0.008
ENSG00000147459	<i>DOCK5</i>	2.026	0.003
ENSG00000136205	<i>TNS3</i>	2.020	0.005
ENSG00000228065	<i>LINC01515</i>	2.016	0.039
ENSG00000130052	<i>STARD8</i>	2.013	0.001
ENSG00000163625	<i>WDFY3</i>	2.007	0.016
ENSG00000157388	<i>CACNA1D</i>	2.005	0.033
ENSG00000139132	<i>FGD4</i>	1.997	0.006
ENSG00000019144	<i>PHLDB1</i>	1.987	0.011
ENSG00000187244	<i>BCAM</i>	1.984	0.024
ENSG00000019991	<i>HGF</i>	1.981	0.019
ENSG00000279091	<i>RP11-461F11.2</i>	1.980	0.023
ENSG00000122778	<i>KIAA1549</i>	1.973	0.029
ENSG00000261634	<i>RP11-352D13.6</i>	1.961	0.020
ENSG00000165186	<i>PTCHD1</i>	1.959	0.025
ENSG00000065833	<i>ME1</i>	1.954	0.002
ENSG00000087842	<i>PIR</i>	1.949	0.015
ENSG00000128805	<i>ARHGAP22</i>	1.941	0.021
ENSG00000266074	<i>BAHCC1</i>	1.941	0.016
ENSG00000184985	<i>SORCS2</i>	1.941	0.042
ENSG00000115919	<i>KYNU</i>	1.938	0.031
ENSG00000142512	<i>SIGLEC10</i>	1.938	0.006
ENSG00000087258	<i>GNAO1</i>	1.935	0.007
ENSG00000147862	<i>NFIB</i>	1.933	0.047
ENSG00000109265	<i>KIAA1211</i>	1.928	0.012
ENSG00000143382	<i>ADAMTSL4</i>	1.923	0.041
ENSG00000139174	<i>PRICKLE1</i>	1.913	0.030
ENSG00000101333	<i>PLCB4</i>	1.912	0.009
ENSG00000182048	<i>TRPC2</i>	1.912	0.028
ENSG00000134755	<i>DSC2</i>	1.908	0.049

(Continued)

**TABLE E1.** (Continued)

Ensembl ID	Associated gene name	Log <sub>2</sub> fold change	q-value
ENSG00000072315	<i>TRPC5</i>	1.906	0.026
ENSG00000115318	<i>LOXL3</i>	1.899	0.029
ENSG00000271086	<i>NAMA</i>	1.898	0.021
ENSG00000060140	<i>STYK1</i>	1.892	0.025
ENSG00000267391	<i>RP11-1151B14.3</i>	1.888	0.010
ENSG00000279440	<i>CTA-992D9.11</i>	1.887	0.036
ENSG00000175274	<i>TP53I11</i>	1.883	0.006
ENSG00000146592	<i>CREB5</i>	1.881	0.034
ENSG00000197430	<i>OPALIN</i>	1.880	0.013
ENSG00000214548	<i>MEG3</i>	1.876	0.046
ENSG00000135083	<i>CCNJL</i>	1.875	0.024
ENSG00000136383	<i>ALPK3</i>	1.875	0.013
ENSG00000173698	<i>ADGRG2</i>	1.873	0.041
ENSG00000183019	<i>MCEMP1</i>	1.872	0.005
ENSG00000147488	<i>ST18</i>	1.863	0.020
ENSG00000169184	<i>MN1</i>	1.858	0.020
ENSG00000233705	<i>SLC26A4-AS1</i>	1.855	0.028
ENSG00000122194	<i>PLG</i>	1.849	0.036
ENSG00000253284	<i>RP11-282K24.3</i>	1.848	0.014
ENSG00000165801	<i>ARHGEF40</i>	1.842	0.008
ENSG00000168916	<i>ZNF608</i>	1.842	0.019
ENSG00000162896	<i>PIGR</i>	1.842	0.041
ENSG00000188580	<i>NKAIN2</i>	1.842	0.014
ENSG00000266805	<i>RP11-61L19.1</i>	1.838	0.008
ENSG00000047936	<i>ROS1</i>	1.832	0.038
ENSG00000012124	<i>CD22</i>	1.831	0.030
ENSG00000140254	<i>DUOXA1</i>	1.831	0.020
ENSG00000103855	<i>CD276</i>	1.823	0.046
ENSG00000110400	<i>PVRL1</i>	1.822	0.004
ENSG00000160293	<i>VAV2</i>	1.819	0.006
ENSG00000111704	<i>NANOG</i>	1.819	0.031
ENSG00000225511	<i>LINC00475</i>	1.810	0.035
ENSG00000132854	<i>KANK4</i>	1.809	0.041
ENSG00000092200	<i>RPGRIP1</i>	1.808	0.031
ENSG00000185559	<i>DLK1</i>	1.807	0.036
ENSG00000136695	<i>IL36RN</i>	1.796	0.039
ENSG00000120318	<i>ARAP3</i>	1.793	0.019
ENSG00000163393	<i>SLC22A15</i>	1.786	0.025
ENSG00000135929	<i>CYP27A1</i>	1.785	0.025
ENSG00000246363	<i>RP11-13A1.1</i>	1.781	0.014
ENSG00000099365	<i>STX1B</i>	1.777	0.014
ENSG00000231064	<i>RP11-263K19.4</i>	1.775	0.009
ENSG00000162390	<i>ACOT11</i>	1.773	0.036
ENSG00000235979	<i>AC004448.5</i>	1.772	0.045
ENSG00000134369	<i>NAV1</i>	1.770	0.009
ENSG00000164330	<i>EBF1</i>	1.767	0.019
ENSG00000114923	<i>SLC4A3</i>	1.767	0.043
ENSG00000130147	<i>SH3BP4</i>	1.767	0.025
ENSG00000122012	<i>SV2C</i>	1.766	0.048
ENSG00000269821	<i>KCNQ1OT1</i>	1.765	0.005
ENSG00000132938	<i>MTUS2</i>	1.762	0.026
ENSG00000170465	<i>KRT6C</i>	1.758	0.037
ENSG00000140090	<i>SLC24A4</i>	1.758	0.011
ENSG00000128408	<i>RIBC2</i>	1.755	0.009
ENSG00000164236	<i>ANKRD33B</i>	1.755	0.012
ENSG00000177519	<i>RPRM</i>	1.755	0.017
ENSG00000146090	<i>RASGEF1C</i>	1.752	0.049
ENSG00000143028	<i>SYPL2</i>	1.750	0.048
ENSG00000167600	<i>CYP2S1</i>	1.750	0.014
ENSG00000095397	<i>DFNB31</i>	1.746	0.008
ENSG00000280169	<i>RP11-151A6.6</i>	1.745	0.028
ENSG00000103067	<i>ESRP2</i>	1.745	0.040

(Continued)

TABLE E1. (Continued)

Ensembl ID	Associated gene name	Log <sub>2</sub> fold change	q-value
ENSG00000134240	<i>HMGCS2</i>	1.741	0.029
ENSG00000134508	<i>CABLES1</i>	1.740	0.007
ENSG00000173801	<i>JUP</i>	1.740	0.011
ENSG00000123307	<i>NEUROD4</i>	1.733	0.042
ENSG00000245526	<i>LINC00461</i>	1.730	0.042
ENSG00000276545	<i>PCDHGB9P</i>	1.730	0.014
ENSG00000221866	<i>PLXNA4</i>	1.729	0.002
ENSG00000130224	<i>LRCH2</i>	1.729	0.030
ENSG00000105711	<i>SCN1B</i>	1.724	0.011
ENSG00000005471	<i>ABCB4</i>	1.723	0.045
ENSG00000168995	<i>SIGLEC7</i>	1.720	0.038
ENSG00000169760	<i>NLGN1</i>	1.720	0.036
ENSG00000269891	<i>ARHGAP19-SLIT1</i>	1.719	0.030
ENSG00000077264	<i>PAK3</i>	1.713	0.009
ENSG00000267065	<i>CTD-2246P4.1</i>	1.711	0.032
ENSG00000149131	<i>SERPING1</i>	1.708	0.048
ENSG00000233393	<i>AP000688.29</i>	1.703	0.029
ENSG00000141519	<i>CCDC40</i>	1.698	0.048
ENSG00000164684	<i>ZNF704</i>	1.697	0.006
ENSG00000136158	<i>SPRY2</i>	1.695	0.003
ENSG00000172421	<i>EFCAB3</i>	1.693	0.016
ENSG00000260105	<i>AOC4P</i>	1.692	0.037
ENSG00000189350	<i>FAM179A</i>	1.691	0.022
ENSG00000133816	<i>MICAL2</i>	1.691	0.001
ENSG00000121753	<i>ADGRB2</i>	1.688	0.044
ENSG00000165376	<i>CLDN2</i>	1.688	0.036
ENSG00000280152	<i>RP11-331F4.5</i>	1.687	0.047
ENSG00000125355	<i>TMEM255A</i>	1.687	0.042
ENSG00000260762	<i>ACSM5P1</i>	1.682	0.043
ENSG00000277837	<i>RP11-714M23.2</i>	1.681	0.044
ENSG00000105251	<i>SHD</i>	1.679	0.026
ENSG00000280474	<i>RP11-216B9.8</i>	1.676	0.010
ENSG00000173406	<i>DAB1</i>	1.674	0.038
ENSG00000171004	<i>HS6ST2</i>	1.672	0.029
ENSG00000114698	<i>PLSCR4</i>	1.670	0.046
ENSG00000170807	<i>LMOD2</i>	1.668	0.025
ENSG00000182791	<i>CCDC87</i>	1.667	0.010
ENSG00000137090	<i>DMRT1</i>	1.665	0.028
ENSG00000115107	<i>STEAP3</i>	1.662	0.030
ENSG00000130182	<i>ZSCAN10</i>	1.661	0.046
ENSG00000171502	<i>COL24A1</i>	1.660	0.028
ENSG00000142798	<i>HSPG2</i>	1.658	0.011
ENSG00000248332	<i>TUB-AS1</i>	1.655	0.032
ENSG00000179604	<i>CDC42EP4</i>	1.649	0.011
ENSG00000228824	<i>MIR4500HG</i>	1.648	0.024
ENSG00000275850	<i>RP11-543P15.3</i>	1.647	0.039
ENSG00000260401	<i>RP11-800A3.4</i>	1.647	0.047
ENSG00000233746	<i>LINC00656</i>	1.644	0.049
ENSG00000181781	<i>ODF3L2</i>	1.642	0.032
ENSG00000279302	<i>RP11-16P20.4</i>	1.641	0.029
ENSG00000233718	<i>MYCNOS</i>	1.640	0.022
ENSG00000087495	<i>PHACTR3</i>	1.638	0.049
ENSG00000170956	<i>CEACAM3</i>	1.637	0.043
ENSG00000204815	<i>TTC25</i>	1.633	0.043
ENSG00000180043	<i>FAM71E2</i>	1.631	0.042
ENSG00000085185	<i>BCORL1</i>	1.629	0.010
ENSG00000161642	<i>ZNF385A</i>	1.629	0.042
ENSG00000167995	<i>BEST1</i>	1.628	0.031
ENSG00000179362	<i>HMG2N2P46</i>	1.627	0.045
ENSG00000137166	<i>FOXP4</i>	1.623	0.026
ENSG00000271776	<i>RP11-52L5.6</i>	1.622	0.034
ENSG00000110243	<i>APOA5</i>	1.622	0.026

(Continued)

TABLE E1. (Continued)

Ensembl ID	Associated gene name	Log <sub>2</sub> fold change	q-value
ENSG00000075651	<i>PLD1</i>	1.621	0.032
ENSG00000282419	<i>TEX13D</i>	1.619	0.046
ENSG00000115386	<i>REG1A</i>	1.617	0.037
ENSG00000143194	<i>MAEL</i>	1.614	0.043
ENSG00000215795	<i>RP11-488L18.3</i>	1.614	0.027
ENSG00000250337	<i>LINC01021</i>	1.613	0.037
ENSG00000103196	<i>CRISPLD2</i>	1.612	0.017
ENSG00000118557	<i>PMFBP1</i>	1.609	0.023
ENSG00000187912	<i>CLEC17A</i>	1.607	0.036
ENSG00000069535	<i>MAOB</i>	1.606	0.049
ENSG00000175866	<i>BAIAP2</i>	1.600	0.011
ENSG00000224687	<i>RASAL2-AS1</i>	1.598	0.025
ENSG00000148600	<i>CDHR1</i>	1.597	0.049
ENSG00000118276	<i>B4GALT6</i>	1.597	0.028
ENSG00000280160	<i>RP11-196G11.3</i>	1.591	0.028
ENSG00000279525	<i>GS1-306C12.1</i>	1.591	0.047
ENSG00000128422	<i>KRT17</i>	1.590	0.049
ENSG00000198722	<i>UNC13B</i>	1.587	0.049
ENSG00000167601	<i>AXL</i>	1.586	0.035
ENSG00000127324	<i>TSPAN8</i>	1.585	0.049
ENSG00000229670	<i>PKP4P1</i>	1.584	0.028
ENSG00000260672	<i>RP11-1006G14.1</i>	1.581	0.034
ENSG00000148143	<i>ZNF462</i>	1.580	0.008
ENSG00000226741	<i>CTA-929C8.6</i>	1.580	0.044
ENSG00000230392	<i>RP5-1139I1.1</i>	1.577	0.048
ENSG00000120162	<i>MOB3B</i>	1.573	0.020
ENSG00000185250	<i>PPIL6</i>	1.572	0.040
ENSG00000227582	<i>ADGRF5P1</i>	1.567	0.050
ENSG00000179059	<i>ZFP42</i>	1.567	0.042
ENSG00000180914	<i>OXTR</i>	1.561	0.046
ENSG00000084731	<i>KIF3C</i>	1.560	0.004
ENSG00000123411	<i>IKZF4</i>	1.560	0.012
ENSG00000189001	<i>SBSN</i>	1.558	0.032
ENSG00000188425	<i>NANOS2</i>	1.557	0.039
ENSG00000066923	<i>STAG3</i>	1.557	0.026
ENSG00000238160	<i>AC116366.5</i>	1.556	0.017
ENSG00000153714	<i>LURAPIL</i>	1.556	0.014
ENSG00000240423	<i>LINC00636</i>	1.554	0.040
ENSG00000163803	<i>PLB1</i>	1.553	0.047
ENSG00000175946	<i>KLHL38</i>	1.550	0.049
ENSG00000151458	<i>ANKRD50</i>	1.547	0.008
ENSG00000072840	<i>EVC</i>	1.545	0.030
ENSG00000156298	<i>TSPAN7</i>	1.543	0.044
ENSG00000256269	<i>HMBS</i>	1.538	0.018
ENSG00000149289	<i>ZC3H12C</i>	1.533	0.020
ENSG00000061492	<i>WNT8A</i>	1.533	0.042
ENSG00000179219	<i>LINC00311</i>	1.531	0.047
ENSG00000279118	<i>RP11-517I3.2</i>	1.526	0.049
ENSG00000121297	<i>TSHZ3</i>	1.525	0.029
ENSG00000189420	<i>ZFP92</i>	1.522	0.025
ENSG00000101236	<i>RNF24</i>	1.517	0.000
ENSG00000198445	<i>CCT8L2</i>	1.516	0.041
ENSG00000172146	<i>OR1A1</i>	1.516	0.040
ENSG00000147912	<i>FBXO10</i>	1.515	0.021
ENSG00000105245	<i>NUMBL</i>	1.514	0.028
ENSG00000280953	<i>LINC01163</i>	1.510	0.025
ENSG00000245385	<i>RP11-334E6.10</i>	1.501	0.039
ENSG00000281955	<i>RP11-126O22.9</i>	1.494	0.027
ENSG00000273267	<i>RP11-338K13.1</i>	1.494	0.019
ENSG00000128487	<i>SPECC1</i>	1.493	0.005
ENSG00000224675	<i>AC009227.2</i>	1.493	0.038
ENSG00000108352	<i>RAPGEFL1</i>	1.490	0.020

(Continued)

TABLE E1. (Continued)

Ensembl ID	Associated gene name	Log <sub>2</sub> fold change	q-value
ENSG00000247982	<i>LINC00926</i>	1.488	0.021
ENSG00000214107	<i>MAGEB1</i>	1.485	0.039
ENSG00000091436	<i>AC013461.1</i>	1.479	0.004
ENSG00000206561	<i>COLQ</i>	1.479	0.003
ENSG00000215562	<i>CNN2P7</i>	1.475	0.041
ENSG00000197879	<i>MYO1C</i>	1.473	0.000
ENSG00000259807	<i>RP11-426C22.4</i>	1.472	0.045
ENSG00000071246	<i>VASH1</i>	1.466	0.032
ENSG00000277639	<i>RP11-295M3.4</i>	1.465	0.030
ENSG00000215455	<i>KRTAP10-1</i>	1.459	0.044
ENSG00000108509	<i>CAMTA2</i>	1.456	0.004
ENSG00000257790	<i>EIF4A1P4</i>	1.453	0.030
ENSG00000241288	<i>RP11-379B18.5</i>	1.450	0.036
ENSG00000280105	<i>RP11-334E15.1</i>	1.445	0.039
ENSG00000188818	<i>ZDHHC11</i>	1.445	0.019
ENSG00000266830	<i>CTD-2008P7.8</i>	1.440	0.045
ENSG00000107159	<i>CA9</i>	1.438	0.049
ENSG00000256812	<i>CAPNS2</i>	1.435	0.045
ENSG00000125741	<i>OPA3</i>	1.433	0.000
ENSG00000236651	<i>DLX2-AS1</i>	1.429	0.026
ENSG00000280140	<i>RP11-597D13.2</i>	1.426	0.035
ENSG00000126705	<i>AHDC1</i>	1.422	0.049
ENSG00000072062	<i>PRKACA</i>	1.411	0.014
ENSG00000088808	<i>PPP1R13B</i>	1.408	0.002
ENSG00000146426	<i>TIAM2</i>	1.405	0.025
ENSG00000106069	<i>CHN2</i>	1.397	0.037
ENSG00000110446	<i>SLC15A3</i>	1.390	0.034
ENSG00000103404	<i>USP31</i>	1.376	0.006
ENSG00000088854	<i>C20orf194</i>	1.373	0.001
ENSG00000090020	<i>SLC9A1</i>	1.369	0.005
ENSG00000255027	<i>RP11-680F20.9</i>	1.364	0.048
ENSG00000123643	<i>SLC36A1</i>	1.355	0.029
ENSG00000087903	<i>RFX2</i>	1.336	0.028
ENSG00000130518	<i>KIAA1683</i>	1.326	0.035
ENSG00000079819	<i>EPB41L2</i>	1.314	0.020
ENSG00000122335	<i>SERAC1</i>	1.309	0.039
ENSG00000127527	<i>EPS15L1</i>	1.295	0.008
ENSG00000103005	<i>USB1</i>	1.287	0.013
ENSG00000004866	<i>ST7</i>	1.282	0.027
ENSG00000104885	<i>DOT1L</i>	1.278	0.028
ENSG00000105556	<i>MIER2</i>	1.270	0.043
ENSG00000173517	<i>PEAK1</i>	1.250	0.046
ENSG00000132024	<i>CC2D1A</i>	1.223	0.031
ENSG00000105771	<i>SMG9</i>	1.218	0.003
ENSG00000138002	<i>IFT172</i>	1.211	0.045
ENSG00000100124	<i>ANKRD54</i>	1.198	0.003
ENSG00000196663	<i>TECPR2</i>	1.187	0.023
ENSG00000011021	<i>CLCN6</i>	1.150	0.021
ENSG00000101152	<i>DNAJC5</i>	0.894	0.033
ENSG00000082153	<i>BZW1</i>	0.888	0.045
ENSG00000079246	<i>XRCC5</i>	0.886	0.039
ENSG00000014824	<i>SLC30A9</i>	0.884	0.003
ENSG00000154473	<i>BUB3</i>	0.876	0.012
ENSG00000136156	<i>ITM2B</i>	0.876	0.013
ENSG00000120910	<i>PPP3CC</i>	0.871	0.002
ENSG00000188243	<i>COMMD6</i>	0.863	0.046
ENSG00000205581	<i>HMGNI</i>	0.860	0.033
ENSG00000165678	<i>GHITM</i>	0.859	0.040
ENSG00000145779	<i>TNFAIP8</i>	0.857	0.032
ENSG00000158773	<i>USF1</i>	0.857	0.017
ENSG00000172340	<i>SUCLG2</i>	0.852	0.009
ENSG00000149100	<i>EIF3M</i>	0.850	0.010

(Continued)

TABLE E1. (Continued)

Ensembl ID	Associated gene name	Log <sub>2</sub> fold change	q-value
ENSG00000165916	<i>PSMC3</i>	0.846	0.014
ENSG00000067955	<i>CBFB</i>	0.836	0.021
ENSG00000198081	<i>ZBTB14</i>	0.828	0.012
ENSG00000168288	<i>MMADHC</i>	0.817	0.028
ENSG00000251791	<i>SCARNA6</i>	0.811	0.044
ENSG00000205531	<i>NAP1L4</i>	0.811	0.022
ENSG00000114125	<i>RNF7</i>	0.806	0.003
ENSG00000255302	<i>EID1</i>	0.796	0.010
ENSG00000252010	<i>SCARNA5</i>	0.795	0.035
ENSG00000137504	<i>CREBZF</i>	0.782	0.002
ENSG00000207297	<i>SNORD7</i>	0.641	0.036

**TABLE E2.** Eighty-nine differentially expressed genes in univariate and multivariate analysis

Ensembl ID	Associated gene name	Log <sub>2</sub> fold change	q-value
ENSG00000179869	<i>ABCA13</i>	2.662	0.0000
ENSG00000165914	<i>TTC7B</i>	2.658	0.0000
ENSG00000168453	<i>HR</i>	2.600	0.0000
ENSG00000136367	<i>ZFH2</i>	2.452	0.0001
ENSG00000109265	<i>KIAA1211</i>	2.363	0.0001
ENSG00000134755	<i>DSC2</i>	2.256	0.0005
ENSG00000204764	<i>RANBP17</i>	2.252	0.0003
ENSG00000196878	<i>LAMB3</i>	2.137	0.0005
ENSG00000147488	<i>ST18</i>	2.043	0.0012
ENSG00000189350	<i>FAM179A</i>	2.039	0.0000
ENSG00000148053	<i>NTRK2</i>	2.030	0.0015
ENSG00000266074	<i>BAHCC1</i>	2.004	0.0004
ENSG00000162390	<i>ACOT11</i>	1.999	0.0007
ENSG00000121753	<i>ADGRB2</i>	1.985	0.0003
ENSG00000152104	<i>PTPN14</i>	1.896	0.0025
ENSG00000116962	<i>NID1</i>	1.882	0.0030
ENSG00000157388	<i>CACNA1D</i>	1.868	0.0024
ENSG00000137135	<i>ARHGEF39</i>	1.851	0.0017
ENSG0000019144	<i>PHLDB1</i>	1.846	0.0008
ENSG00000163393	<i>SLC22A15</i>	1.835	0.0020
ENSG00000156298	<i>TSPAN7</i>	1.751	0.0106
ENSG00000267065	<i>CTD-2246P4.1</i>	1.738	0.0112
ENSG00000115919	<i>KYNU</i>	1.717	0.0025
ENSG00000117115	<i>PADI2</i>	1.707	0.0017
ENSG00000215795	<i>RP11-488L18.3</i>	1.689	0.0120
ENSG00000073464	<i>CLCN4</i>	1.689	0.0032
ENSG00000135083	<i>CCNJL</i>	1.686	0.0151
ENSG00000115318	<i>LOXL3</i>	1.664	0.0152
ENSG00000163803	<i>PLB1</i>	1.649	0.0014
ENSG00000153714	<i>LURAP1L</i>	1.638	0.0180
ENSG00000087842	<i>PIR</i>	1.614	0.0209
ENSG00000122012	<i>SV2C</i>	1.612	0.0196
ENSG00000276545	<i>PCDHGB9P</i>	1.572	0.0229
ENSG00000135636	<i>DYSF</i>	1.565	0.0164
ENSG00000269821	<i>KCNQ1OT1</i>	1.563	0.0016
ENSG00000173406	<i>DAB1</i>	1.554	0.0166
ENSG00000246363	<i>RP11-13A1.1</i>	1.554	0.0209
ENSG00000103067	<i>ESRP2</i>	1.543	0.0293
ENSG00000155754	<i>ALS2CR11</i>	1.505	0.0339
ENSG00000118557	<i>PMFBP1</i>	1.486	0.0097
ENSG00000113657	<i>DPYSL3</i>	1.483	0.0368
ENSG00000139132	<i>FGD4</i>	1.453	0.0089
ENSG00000214548	<i>MEG3</i>	1.452	0.0417
ENSG00000169184	<i>MN1</i>	1.432	0.0376
ENSG00000122778	<i>KIAA1549</i>	1.430	0.0311
ENSG00000174099	<i>MSRB3</i>	1.427	0.0120
ENSG00000130224	<i>LRCH2</i>	1.398	0.0464
ENSG00000180914	<i>OXTR</i>	1.393	0.0428
ENSG00000174059	<i>CD34</i>	1.390	0.0284
ENSG00000118276	<i>B4GALT6</i>	1.370	0.0220
ENSG00000075651	<i>PLD1</i>	1.362	0.0189
ENSG00000112414	<i>ADGRG6</i>	1.350	0.0276
ENSG00000167995	<i>BEST1</i>	1.348	0.0293
ENSG00000136854	<i>STXBP1</i>	1.347	0.0173
ENSG00000110400	<i>PVRL1</i>	1.342	0.0092
ENSG00000185250	<i>PPIL6</i>	1.333	0.0358
ENSG00000160293	<i>VAV2</i>	1.332	0.0126
ENSG00000140090	<i>SLC24A4</i>	1.327	0.0305
ENSG00000130147	<i>SH3BP4</i>	1.310	0.0311
ENSG00000134369	<i>NAV1</i>	1.305	0.0205

(Continued)

**TABLE E2.** (Continued)

Ensembl ID	Associated gene name	Log <sub>2</sub> fold change	q-value
ENSG00000175274	<i>TP53I11</i>	1.298	0.0214
ENSG00000142512	<i>SIGLEC10</i>	1.291	0.0307
ENSG00000165801	<i>ARHGEF40</i>	1.286	0.0346
ENSG00000066923	<i>STAG3</i>	1.284	0.0103
ENSG00000142798	<i>HSPG2</i>	1.277	0.0091
ENSG00000105245	<i>NUMBL</i>	1.243	0.0150
ENSG00000106069	<i>CHN2</i>	1.220	0.0183
ENSG00000167601	<i>AXL</i>	1.216	0.0499
ENSG00000085185	<i>BCORL1</i>	1.187	0.0193
ENSG00000164684	<i>ZNF704</i>	1.179	0.0274
ENSG00000171502	<i>COL24A1</i>	1.178	0.0402
ENSG00000221866	<i>PLXNA4</i>	1.168	0.0109
ENSG00000189420	<i>ZFP92</i>	1.151	0.0311
ENSG00000175866	<i>BAIAP2</i>	1.126	0.0213
ENSG00000147459	<i>DOCK5</i>	1.101	0.0349
ENSG00000072840	<i>EVC</i>	1.081	0.0444
ENSG00000095397	<i>DFNB31</i>	1.004	0.0485
ENSG00000179604	<i>CDC42EP4</i>	0.966	0.0129
ENSG00000108352	<i>RAPGEFL1</i>	0.917	0.0478
ENSG00000128487	<i>SPECC1</i>	0.899	0.0066
ENSG00000133816	<i>MICAL2</i>	0.897	0.0175
ENSG00000084731	<i>KIF3C</i>	0.893	0.0191
ENSG00000198752	<i>CDC42BPB</i>	0.873	0.0229
ENSG00000091436	<i>AC013461.1</i>	0.792	0.0353
ENSG00000206561	<i>COLQ</i>	0.772	0.0406
ENSG00000088808	<i>PPP1R13B</i>	0.642	0.0205
ENSG00000101236	<i>RNF24</i>	0.573	0.0287
ENSG00000125741	<i>OPA3</i>	0.568	0.0114
ENSG00000077264	<i>PAK3</i>	0.538	0.0014